Supplementary information

Electrohydrodynamic removal of non-specific colloidal adsorption at electrode interfaces

Sakandar Rauf,[a] Muhammad J. A. Shiddiky*[a] and Matt Trau*[a,b]

[a]Australian Institute for Bioengineering and Nanotechnology (AIBN), The University of Queensland, Corner of College and Coopers Roads, Brisbane, QLD 4072, Australia. [b]School of Chemistry and Molecular Biosciences, University of Queensland, Brisbane, QLD 4072, Australia E-mail: m.shiddiky@uq.edu.au and m.trau@uq.edu.au:

1. Materials

Cysteamine hydrochloride and EZ-Link sulfo-NHS-LC-biotin were purchased from Sigma-Aldrich, Australia and Thermo scientific, Australia, respectively. Streptavidin coated dragon green fluorescent microspheres of average size 1.04 μm (zeta potential (ζ) = -21.5 ± 4.67) and carboxyl functionalized suncoast yellow fluorescent microspheres of average size 0.97 μm (zeta potential (ζ) = -65.0 ± 7.25) were purchased from Bangs laboratories, Inc. 1 mM phosphate buffered saline (PBS) was prepared using the buffer tablets obtained from Sigma-Aldrich, Australia.

2. Fabrication of the devices

Figure S1 shows the fabrication process of the devices used in these studies. Pyrex glass wafers (4", 1 mm thick, double-side polished) were obtained from Bonda technology, Singapore and sodalime chrome masks (5" X 5") were obtained from Qingyi Precision Maskmaking (Shenzhen) Ltd, China. The microdevices were designed using Layout Editor (L-Edit V15, Tanner Research Inc., CA). Before photolithography, the glass wafers were cleaned by sonication in acetone and Isopropanol (IPA) and dried under flow of nitrogen gas. The devices were fabricated in two photolithography steps. In the first step, the cleaned glass wafers were coated with positive photoresist (AZ9260 Microchemicals, Germany) to obtain a ~7 μm thick resist layer (4000 rpm for 60s), followed by a soft bake for 7 min at 110 ºC. The positive photoresist coated wafers were then UV exposed (1000 mJ/cm^2) using a mask aligner (EVG620, EV Group GmbH, Austria) and developed in AZ 726 developer solution (Microchemicals, Germany) for 8 min, followed by rinsing with deionized (DI) water (Millipore Pvt. Ltd., Australia) and dried under the flow of nitrogen gas. The wafers were

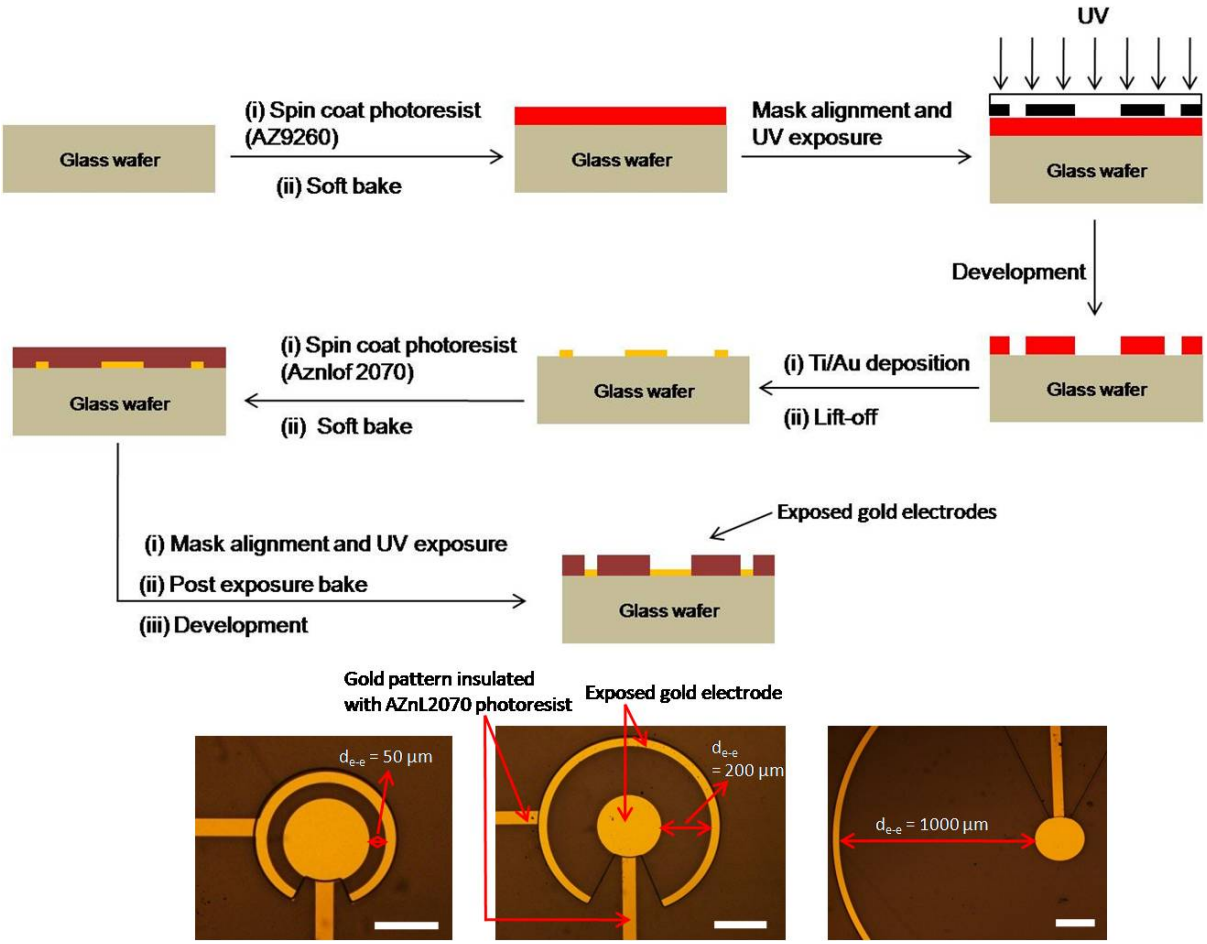

Fig. S1 (A) Schematic representation of the fabrication of asymmetric electrodes pairs. (B) Brightfield images of the fabricated electrodes (from left to right 50, 200 and 1000 µm edge to edge distance between inner and outer electrode = d_{e-e}). The diameter of the inner circular electrode is 250 µm. The width of the outer ring electrodes is 30 µm. The scale bar is 200 µm.

then treated with oxygen plasma (60 watt for 45s) to remove any residual resist layer in the developed patterns. The gold deposition (10 nm of titanium as adhesion layer followed by 200 nm of gold layer) was done using an e-beam evaporator (Temescal BJD-2000 E-beam). Finally, the asymmetric pair of gold electrodes were obtained via the acetone lift-off process. In each design, the inner circular electrode has the same diameter i.e. 250 µm and width of the outer ring electrode was 30 µm. The size (i.e., geometric area) of the outer electrode was controlled by the distance between the inner and outer electrode (edge to edge distance between inner and outer electrode = d_{e-e}) which is 50 µm, 200 µm and 1000 µm. These electrodes were connected with the ac signal generator via the large gold connecting pads of

7×2 mm^2 and work as cathode or anode of an electrolytic cell during the ac-EHD experiments.

In the second lithography step, the gold electrodes were coated with a negative photoresist (AZnL2070, Microchemicals, Germany) at 3000 rpm for 30s to obtain ~7μm thick resist layer. After soft baking at 110ºC for 3min, the wafers were exposed using the mask aligner and developed in AZ 726 developer solution to expose the gold electrodes and connecting pads. All other areas of the devices were covered with the resist layer (i.e., working area of the electrodes is only exposed to solution). The geometric area or working area of the inner circular electrode was 4.9×10^4 μm^2. The geometric areas of the outer electrodes with $d_{e\text{-}e}$ =1000, 200 and 50 μm were found to be 2.1×10^5, 6.4×10^4 and 3.5×10^4 μm^2 , respectively. The wafers were then diced into individual devices using a dicing machine (ADT-7100). Before using the devices, an oxygen plasma cleaning (100 watts, 45s) was performed to remove any residual resist particles present on the electrode surface.

3. Real-time fluorescence measurements

In these measurements, a Nikon eclipse fluorescence microscope equipped with a dual band pass filter set (ET-FITC/CY3) and a high speed colour CCD camera was used in order to observe green and red fluorescent beads simultaneously. A PDMS spacer of ~0.4 mm thick having 5 mm hole in the centre was placed on top of the electrode pair, which defines the volume of the working chamber. In each experiment 15 μL of the solution was dropped on the electrode and covered with a glass coverslip to seal the chamber. The glass cover slip allows us to view the underlying electrodes with microscope objective. The device was then connected to a signal generator (Agilent 33510B waveform Generator, Agilent Technologies, Inc., CA) via gold connecting pads and a BNC connector to apply ac electric field. Biotinylated gold electrodes were used to capture strepatvidin coated beads. Briefly, the electrodes were initially incubated overnight at room temperature in 10 mM aqueous solution of cysteamine hydrochloride. After washing with plenty of de-ionized water electrodes were dry under a flow of nitrogen gas. These electrodes were then incubated in 3 mg/mL solution of EZLink sulfo-NHS-LC-biotin in 10 mM PBS pH 7.4 for 3h. To remove any unbound EZLink sulfo-NHS-LC-biotin, these electrodes were washed three times with PBS solution.

In this study, the streptavidin coated dragon green fluorescent and carboxyl functionalized suncoast yellow fluorescent microspheres were used as specific and non-specific beads, respectively. Designated percentages of the specific and non-specific beads were used to make mixture solutions with designated amounts of green and red colour beads as shown in Table 1. The total number of beads per ml (2×10^9) was kept constant for all the mixtures. The bead solutions were prepared in 1 mM PBS (i.e., 1 mM NaH_2PO_4, 1 mM Na_2HPO_4, and 13.7

Formulation	Specific (%)	Non-specific (%)
1	0	100
2	25	75
3	50	50
4	75	25
5	100	0

Table. 1. Percentage of different mixtures of beads used in the experiments.

mM NaCl). Only 15 µL of this mixture was dropped on the electrode surface. The ac field was applied under different frequency (f) and amplitude (V_{pp}) and movement/ attachment of the beads was observed in real time using a fluorescence microscope equipped with a high speed colour CCD camera.

In order to calculate the velocity of the particles under different peak to peak voltages, frequency and salt concentrations, NIH Image J software was used to calculate the average maximum velocity of the particles (µm/s) from the videos (-COOH labelled beads) taken at different conditions. It was found that with the increase in frequency from 25 Hz to 500 Hz, the average maximum velocity (average of thirty beads in each case) was attained at a field strength of f = 100 Hz (120 µm/s) at constant V_{pp} = 4V and 10 mM KCl, whilst the velocity tends to drop at 250 Hz and 500Hz in case of $d_{e\text{-}e}$ = 1000 µm (data not shown). After 500 Hz, the beads demonstrated Brownian motion indicating no movement at higher frequencies. In case of different voltages, it was found that at a constant frequency f = 100 Hz and in 10 mM KCl, the lowest velocity was observed at 3V (25 µm/s) and found to increase at 4V (120 µm/s) and 5V (133 µm/s) (data not shown). However, it is important to note that in case of amplitude equal or greater than 5V, the electrode was damaged within one minute of operation and remained intact under lower amplitudes ($\leq$ 4V).

We also calculated the velocity of the particles at different salt concentrations (1mM to 50mM KCl) at fixed frequency (100Hz) and amplitude (4V). The velocity of the particles was found to increase from 1mM to 10mM and then decrease at concentrations of 20 and 30mM (data not shown). Beyond 30mM, the electrode surface was damaged rapidly making it impossible to observe any fluid flow.

4. Real time observation of electrohydrodynamic effect

Fig. S2 Video 1 shows the specific capture of streptavidin beads and displacement of non-specific carboxyl beads in real time at the field strength of f = 100 Hz and V_{pp} = 4 V. The central electrode diameter = 250 μm and edge to edge spacing between inner and outer electrode ($d_{e\text{-}e}$) = 1000 μm.

5. Control experiments

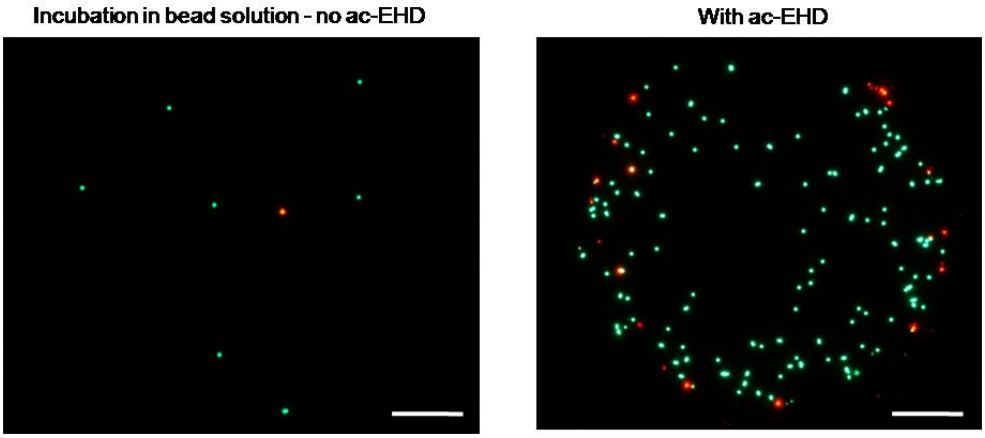

Fig. S3 Shows the comparison between biotin modified electrodes for specific capture of streptavidin beads with or without ac-EHD (incubation in bead solution). The beads mixture was 50% specific and 50% non-specific. The incubation time in case of without ac-EHD was 24 h. The ac field strength of f = 100 Hz and V_{pp} = 4 V was applied for 5 min. The scale bar is 50 μm.

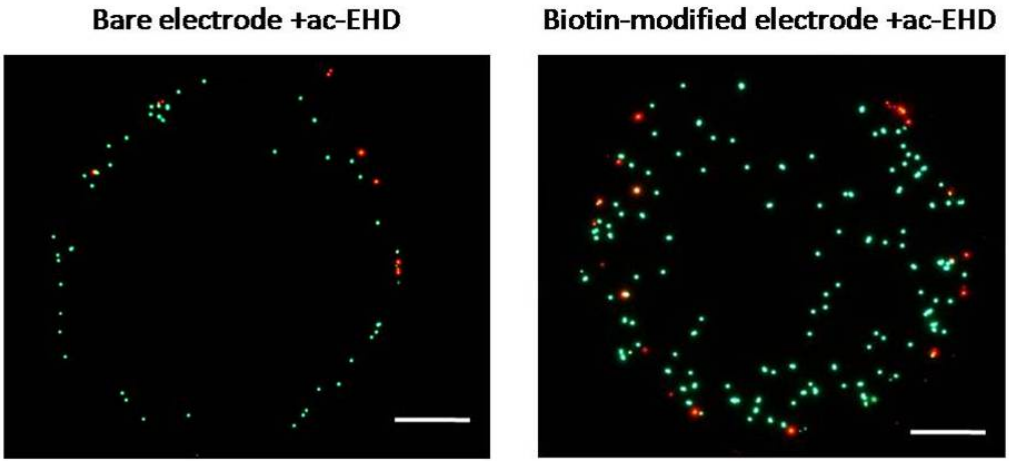

Fig. S4 Shows the comparison between the unmodified (bare) and biotin modified electrodes for specific capture of streptavidin beads in the presence of -COOH modified beads (50% specific + 50% non-specific). The ac field strength of f = 100 Hz and V_{pp} =4 V. The scale bar is 50 μm.

6. Effect of different frequencies

Figure S5 shows the frequency dependence of the specific capture of streptavidin beads in the presence of non-specific -COOH beads. It can be seen that at a frequency of 100 Hz and constant V_{pp} = 4V, the capture of streptavidin was more efficient whilst at higher frequencies (250 and 500 Hz) there was a decrease in specific capture and also an increase in the level of non-specific bead adsorption onto the electrode surface. The resulting high level of capture at low frequency (100 Hz) is probably due to the stimulation of the fluid flow around the biotin-functionalized electrodes, which can maximize the effective beads (beads are streptavidin functionalized)-biotin collisions (a condition where shear force < beads-biotin binding force) while these forces were strong enough to displace the weakly bound non-specific (-COOH) beads.

However, at frequencies higher than 100Hz, the corresponding bead velocities at 250 Hz and 500 Hz were smaller than the bead velocities at 100 Hz. At higher frequencies, the decrease in applied potential across the electrolyte leads to significant drop in the amount of induced charges in the double layer.[1, 2] Therefore, both streptavidin and -COOH beads move slowly at higher frequencies (250 Hz and 500 Hz) and are adsorbed on the electrode surface without

any specific attachment to the electrode surface. This resulted in higher non-specific adsorption of the -COOH beads as shown in Fig. S5.

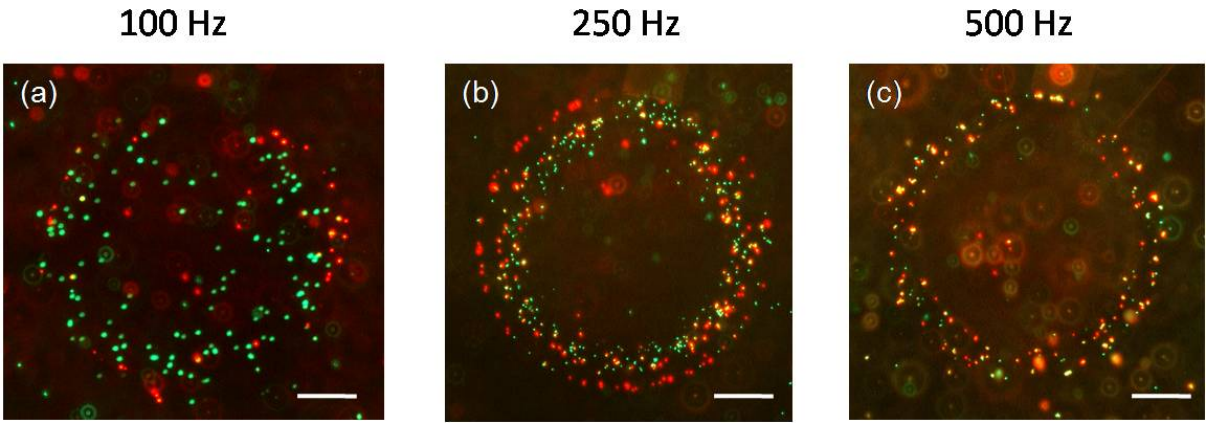

Fig. S5 Effect of the ac frequency on electrohydrodynamic removal of non phenomenon. The snapshots of the middle electrode were taken from real-time videos (see videos 2-4) after 5 min operation of the device under the frequency of (a) 100 Hz, (b) 250 Hz, and (c) 500 Hz at constant amplitude of 4 V. The scale bar is 50 μm.

7. Effect of spacing between the asymmetric electrodes

Figure S6 shows the effect of spacing on the capture efficiency of a mixture solution (50% specific and 50% non-specific) under the same applied field strength (f = 100 Hz and V_{pp} = 4 V). It can be seen that the electrode geometry with $d_{e\text{-}e}$= 1000 μm resulted in better capture efficiency and removal of non-specific beads as compared to devices with $d_{e\text{-}e}$ of 50 and 200 μm. This may be due to the larger lateral variation in the total amount of double layer charges and spatial distribution of charges on electrode pairs in devices with $d_{e\text{-}e}$ =1000 μm compared to the devices with $d_{e\text{-}e}$ = 50 μm and 200 μm. The resultant non-uniform force due to induced charges on the larger electrode is stronger than that on the smaller electrode, resulting in a lateral flow towards the large electrode (in this case the outer ring electrode). The steady flow towards the larger electrode causes any beads in solution to be dragged by the flow, and provide pronounced fluid mixing and effective surface shear forces that allow more effective binding of the streptavidin beads over non-specific -COOH beads.

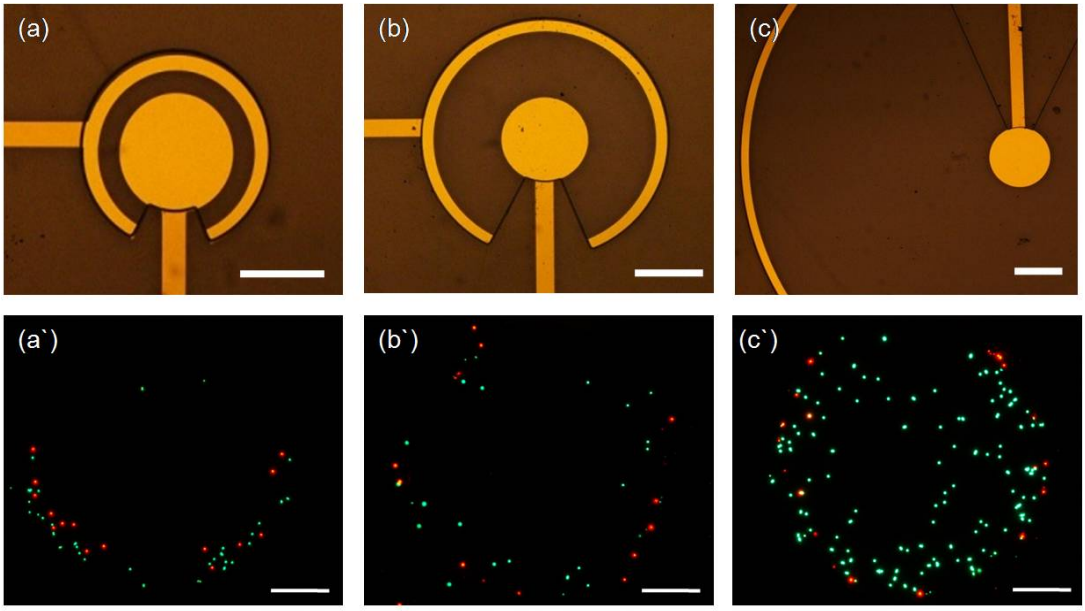

Fig. S6 Brightfield microscopic images of different asymmetric electrodes pairs with $d_{e\text{-}e}$ of (a) 50, (b) 200, and (c) 1000 µm. The diameter of the central electrode and thickness of the outer ring electrode in all cases is 250 and 30 µm, respectively. The scale bar is 200 µm. Corresponding (a', b' and c') capture efficiency for a mixture solution (50% specific and 50% non-specific) of beads under the field strength of f = 100 Hz and V_{pp} = 4 V. The scale bar is 50 µm.

Videos for three images are shown in Videos 2, 5 and 6. Notably, in case of device with the $d_{e\text{-}e}$ of 50 µm (video 5) fluid flows in opposite direction (i.e., toward inner circular electrode) to that of the device with $d_{e\text{-}e}$ of 200 or 1000 µm. This is because the effective area of the inner circular electrode is larger than that of the outer ring electrode, which drives the bulk fluid motion towards the larger electrode (as explained in the main text).

Fig. S7 Videos 2 and 7-10 shows the specific capture of streptavidin beads and displacement of non-specific carboxyl beads in real time at the field strength of f = 100 Hz and V_{pp} = 4 V. The central electrode diameter = 250 µm and edge to edge spacing between inner and outer electrode ($d_{e\text{-}e}$) = 1000 µm. Video 7= 100% non-specific beads, video 8 = 75% non-specific

beads + 25% specific beads, video 2= 50% non-specific beads + 50% specific beads, video 9= 25% non-specific beads + 75% specific beads and video 10= 100% specific beads.

References

1. A. Ramos, H. Morgan, N. G. Green and A. Castellanos, *J Colloid Interface Sci*, 1999, 217, 420-422.

2. C. C. Wu and D. J. Yang, *Biosens Bioelectron*, 2013, 43, 348-354.